The "Invisible" ^{13}C NMR Chemical Shift of the Central Carbon Atom in $[(Ph_3PAu)_6C]^{2+}$: A Theoretical Investigation

Boris Le Guennic,[a, d] Johannes Neugebauer,[b, c] Markus Reiher,[b, d] and Jochen Autschbach*[a]

In memory of Professor Bernd Artur Hess who passed away on July 17, 2004

Abstract: The experimental ^{13}C NMR chemical shift of the central carbon atom in the octahedral $[(Ph_3PAu)_6C]^{2+}$ cluster was investigated on the basis of relativistic density functional calculations. In order to arrive at independent model conclusions regarding the value of the chemical shift, a systematic study of the dependence of the cluster structure on the phosphine ligands, the chosen density functionals, and the basis set size was conducted. The best structures obtained were then used in the NMR calculations. Because of the cage-like cluster structure a pronounced deshielding of the central carbon nucleus could have been expected. However, upon comparison with the ^{13}C NMR properties of the related complex $[C\{Au[P(C_6H_5)_2(p\text{-}C_6H_4NMe_2)]\}_6]^{2+}$, Schmidbaur et al. have assigned a signal at $\delta = 135.2$ ppm to the interstitial carbon atom. Our calculations confirm this value in the region of the aromatic carbon atoms of the triphenylphosphine ligands. The close-lying signals of the 108 phenyl carbon atoms can explain the difficulties of assigning them experimentally.

Keywords: cluster compounds · density functional calculations · gold · NMR spectroscopy · relativistic effects

Introduction

The fascinating octahedral gold cluster $[(Ph_3PAu)_6C]^{2+}$ (**1**) was synthesized by Schmidbaur et al. in 1988 and extensively investigated by single crystal X-ray diffraction and NMR spectroscopy.[1] Its structure is depicted in Figure 1. Since it has a six-coordinated carbon atom inside the Au_6 cage one would expect unusual NMR parameters. Cage-like clusters can exhibit a pronounced effect on the NMR chemical shift of interstitial atoms; one example is the extraordinarily large ^{183}W chemical shielding that has been recently predicted for the WAu_{12} cluster.[2] On the other hand, in interstitial carbides ^{13}C nuclei are known to be very strongly deshielded. Other examples are the ^{13}C NMR chemical shifts of a series of interstitial carbides in transition-metal clusters.[3–7] It might thus be expected that the interstitial ^{13}C NMR chemical shift in **1** is very large in magnitude, either positive or negative depending on whether the chemical environment is similar to carbides or similar to clusters as WAu_{12}.

[a] Dr. B. Le Guennic, Dr. J. Autschbach
Department of Chemistry
312 Natural Sciences Complex
State University of New York at Buffalo
Buffalo, NY 14260-3000 (USA)
Fax: (+1) 716-645-6963
E-mail: jochena@buffalo.edu

[b] Dr. J. Neugebauer, Dr. M. Reiher
Lehrstuhl für Theoretische Chemie
Universität Erlangen, Egerlandstrasse 3
91058 Erlangen (Germany)

[c] Dr. J. Neugebauer
Present address: Theoretical Chemistry
Vrije Universiteit Amsterdam, De Boelelaan 1083
1081 HV Amsterdam (The Netherlands)

[d] Dr. B. Le Guennic, Dr. M. Reiher
Present address: Lehrstuhl für Theoretische Chemie der Universität Bonn, Wegelerstrasse 12
53115 Bonn (Germany)

Supporting information for this article is available on the WWW under http://www.chemeurj.org/ or from the author: Optimized structures (Cartesian coordinates) for the complexes $[(Ph_3PAu)_6C]^{2+}$ (**1**), $[C\{Au[P(C_6H_5)_2(p\text{-}C_6H_4NMe_2)]\}_6]^{2+}$ (**2**) and $[(iPr_3PAu)_6C]^{2+}$ (**4**).

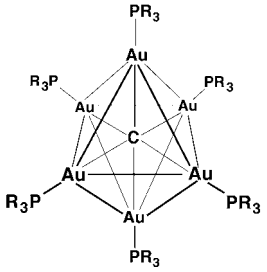

Figure 1. Structure of the $[(R_3PAu)_6C]^{2+}$ clusters.

 DOI: 10.1002/chem.200400317

A number of computational studies have been devoted to the understanding of the origin of the deshielding of interstitial atoms in metal clusters. For instance, Fehlner et al. have performed molecular orbital analyses of the ^{11}B NMR chemical shifts of boride-centered transition-metal carbonyl clusters.[8,9] The ^{13}C chemical shift tensors for interstitial carbides of the previously cited series of transition metal carbonyl clusters have been calculated by Kaupp using sum-over-states density functional perturbation theory.[10] It has been shown that the downfield chemical shifts are related directly to the paramagnetic contribution caused by interstitial carbon–metal bonding. Hughbanks et al. have presented a qualitative analysis of the interstitial chemical shifts of centered hexazirconium halide clusters.[11] By using the density functional theory, a quantitative extension of this work has established additional correlations between the interstitial chemical shifts and the electronic structure of such complexes.[12]

However, previous analyses of the electronic structure of main group element centered octahedral gold clusters have highlighted the differences between the title complex and interstitial carbide complexes.[1,13] In particular, one should underline that the gold systems are thought to have radial C–Au bonds and rather weak (aurophilic) interactions between the AuL ligands, whereas in the case of interstitial carbide complexes, strong metal–metal bonds stabilize the structures.

For the related complex $[C\{Au[P(C_6H_5)_2(p\text{-}C_6H_4NMe_2)]\}_6]^{2+}$ (**2**), Schmidbaur et al. have unambiguously assigned a signal at $\delta = 137.27$ ppm to the interstitial carbon atom.[14] With the δ and J values of this compound, the authors identified a ^{13}C NMR signal at $\delta = 135.2$ ppm in the unsubstituted parent complex **1** as originating from the interstitial carbon. The ^{13}C NMR resonance of this carbon atom appeared in a completely unexpected region, since a strong deshielding was expected: Signals of interstitial carbon atoms in transition metal carbonyl carbides appear as far downfield as $\delta = 450$ ppm.[15] As mentioned by the authors, "an explanation for this discrepancy is only to be expected from theoretical calculations, which, in the case of heavy metals—and especially in the case of gold—must take into account strong relativistic effects."[14] The septuplet signals of the central C atoms of the alkylphosphane-based clusters $[(Et_3PAu)_6C]^{2+}$ (**3**) and $[(iPr_3PAu)_6C]^{2+}$ (**4**) were also easily detected at $\delta = 159.0$ and 154.6 ppm, respectively, due to the absence of phenyl substituents.[16] These signals thus appear about 10 to 15 ppm downfield relative to the complex **1**.

The $[(Ph_3PAu)_6C]^{2+}$ cluster represents a challenging system for any quantum chemical approach. For example, the phosphine ligands contain 18 phenyl rings in total, the effect of which on the molecular and electronic structures is not negligible. Theoretical studies on large clusters comprising heavy atoms require the most elaborate quantum chemical methods. Apart from the nonlinear scaling of quantum chemical methods with the number of electrons, the large nuclear charges of the gold atoms induce sizable relativistic effects, which need to be properly taken into account both in the structure optimizations and in the NMR calculations. Accurate quantum chemical calculations of NMR properties that do not employ scalar relativistic ECPs but a two- or four-component Hamiltonian or spin-orbit ECPs are still rare for large "relativistic" transition-metal compounds.[17–24] Consequently, many open questions regarding the NMR of such systems still remain to be answered.

In a previous study,[25] we have predicted the vibrational frequencies of the $[Au_6C]^{2+}$ moiety of the cluster in the full ligand system. We have been able to quantitatively reproduce the amount of core-ligand vibrational couplings. In contrast to the inherent possibility of vibrations to exhibit non-locality, that is to couple directly with the ligand atoms, NMR chemical shifts are considered local molecular properties. Apart from the yet unknown magnitude of the ^{13}C NMR chemical shift of the central C atom in **1**, the dependence of this shift on the phosphine ligands represents an interesting theoretical problem in itself. The effect of the ligands is twofold. On the one hand, they have a direct electronic influence on the chemical shift and, on the other hand, different substituents in the phosphine ligands will result in different minimum structures of the complex, which will also affect the electronic structure and in turn the chemical shift.

The inherent technical limitations of the applied methods, that is, the density functionals, basis sets, and optimized structures are assessed for three different models of the $[(Ph_3PAu)_6C]^{2+}$ complex: cluster **I** is the bare $[Au_6C]^{2+}$ core, cluster **II** is the simplest model with PH_3 ligands, that is, $[(H_3PAu)_6C]^{2+}$, and cluster **III** is $[(Me_3PAu)_6C]^{2+}$. Finally, we have also studied the experimentally known full clusters $[(Ph_3PAu)_6C]^{2+}$ (**1**), $[C\{Au[P(C_6H_5)_2(p\text{-}C_6H_4NMe_2)]\}_6]^{2+}$ (**2**) and $[(iPr_3PAu)_6C]^{2+}$ (**4**) (see Supporting Information for the optimized structures).

Computational Details

For all structure optimizations we have used the density functional and ab initio programs provided by the Turbomole 5.4 suite.[26] While we have employed the second-order Moller–Plesset (MP2) model for the accurate description[27–31] of the aurophilic attraction, which is a dispersion-type interaction, only DFT methods are feasible for the description of the large clusters **III**, **1**, **2**, and **4**. In the structure optimizations, we have employed the effective core potential from the Stuttgart group[32] as provided by Turbomole for the gold atoms, which has allowed us to treat only 19 electrons per Au atom explicitly (i.e., 5spd and 6s). Apart from the core electrons substituted by the effective core potential, the six molecular orbitals of lowest eigenvalue in the $[Au_6C]$ system were kept frozen in the MP2 calculations. In the DFT calculations, we have used the Becke–Perdew functional (BP86),[33,34] and the Vosko–Wilk–Nusair (VWN)[35] local density approximation (LDA) functional (combined with Slater–Dirac exchange), as implemented in Turbomole. For all DFT and MP2 calculations we have applied the resolution-of-the-identity technique.[36,37] Ahlrichs' TZVP and TZVPP basis sets[38] featuring a valence triple-ζ basis set with polarization functions on all atoms, have been employed in the structure optimizations. According to the method described by Pyykkö et al.,[29] we replaced the f function for Au with exponent 1.056 in the TZVPP basis set by two primitive f functions with exponents

1.19 and 0.2. This replacement is known to have significant effects on structures of gold clusters.[2] Since no auxiliary basis sets of TZVPP or TZVPP(2f) quality are available for Au in Turbomole 5.4, we have used the TZVP auxiliary basis instead. Test calculations showed that this has a negligible effect on the results. For the phenyl (Ph) substituents in the large complexes **1** and **2**, we have employed Ahlrichs' SVP basis set[39] featuring a valence double-ζ basis set with polarization functions on all atoms. The conformation of the PPh_3 ligands in **1** is the same as in the experimental complex.[1]

Relativistic density functional NMR computations have been carried out with the Amsterdam Density Functional (ADF) program package.[40–42] It incorporates the code developed by Wolff et al.[43] for the two-component relativistic computation of nuclear shielding constants, based on the zeroth-order regular approximation (ZORA) Hamiltonian.[44,45] The NMR code has been modified in order to allow a more efficient treatment of larger systems.[46] The modifications that have been made do not affect the results obtained with the program but implement a significantly better scaling of the computational time with increasing system size. It has recently been demonstrated that the ZORA Hamiltonian yields very accurate relativistic hyperfine integrals for the valence orbitals of heavy atoms[47] (see also ref. [48]). The chemical shifts can therefore be expected to be close to fully relativistic DFT NMR results that would otherwise be equivalent in terms of basis functions, exchange-correlation potential, and other parameters that affect the quality of the computation.

As formulated in ref. [43], the shielding constant σ_A for a nucleus A within the relativistic ZORA formalism consists of four terms:

$$\sigma_A = \sigma_A^D + \sigma_A^P + \sigma_A^{SO} + \sigma_A^{GC} \quad (1)$$

Here, σ_A^D is the diamagnetic shielding, and σ_A^P the paramagnetic one. These two terms are also present in a non-relativistic or a scalar (i.e., "one-component relativistic") ZORA calculation. σ_A^{SO} denotes the spin-orbit induced terms due to the ZORA analogues of the Fermi contact (FC) and the spin–dipole (SD) operators.[23] It is important to note that, due to the different shapes of the orbitals obtained from a variational two-component calculation, σ_A^D and σ_A^P are also somewhat different comparing with scalar relativistic calculations. Finally, σ_A^{GC} denotes gauge correction terms obtained from the implemented GIAO (gauge including atomic orbitals)[49–51] formalism in a finite basis. Chemical shifts with respect to a reference nucleus (ref) are calculated as:

$$\delta_A = \sigma_A^{ref} - \sigma_A^{probe} \quad (2)$$

The VWN functional has been used in most NMR computations. It has been shown that it provides a reasonable accuracy for NMR properties of heavy nuclei in "relativistic" systems,[23,46,52–59] but not necessarily for light ligand nuclei. Therefore, NMR chemical shifts have additionally been computed by using the Perdew–Wang (PW91)[60] and the BP86 generalized gradient correction (GGA) density functionals in order to analyze the dependence of the results on the approximations in the density functional.

The influence of the size of the basis sets on the ^{13}C NMR shielding has been studied with several basis sets according to the complexity of the molecules. The Slater-type basis sets that were employed are of triple-ζ quality for valence and outer core shells, augmented with two polarization functions for the gold and the central carbon atoms (TZ2P) and one polarization function for the phosphorus atoms (TZP). The all-electron basis sets are of double-ζ quality for the core shells. In some cases, a core including the shells 1s to 4p has been kept frozen for Au whereas a frozen core including the shells 1s to 2p has always been employed for P. Different basis sets (double- or triple-ξ (DZ or TZ), with or without polarization functions (P)) have been used for the C and H atoms of the phosphine ligands, with a 1s frozen core for the C atoms (see Table 2). In addition, for some computations the central carbon's TZ2P basis has been augmented with an even-tempered set of 1s and 2p Slater functions with exponents a up to about 50 ($\alpha_{n+1}/\alpha_n = 1.35$) starting with the highest exponent close to the nuclear charge Z in the TZ2P basis. For heavy nuclei we have previously applied the same recipe[52,53] but adding functions with exponents up to 5000. The truncation at $\alpha \sim 10^4$ was shown to compensate for some of the finite-nucleus effects (see ref. [52]). For a carbon nucleus, finite-nucleus effects should be negligible. The high-exponent functions for carbon are necessary to provide an accurate description of the perturbation by the Fermi contact (FC) term. We have previously found that truncating the series for α around 50 for 2nd row atoms provides reasonably well converged FC terms in spin–spin coupling constants.[53] In heavier systems, both for the relativistic electronic structure and for the FC term high exponents are needed. We will denote the augmented basis set by aug-TZ2P in the following and already note here that this basis set yields much improved chemical shifts compared with the TZ2P basis.

Chemical shifts are reported with respect to the standard reference tetramethylsilane (TMS). For each chemical shift reported here, the ^{13}C NMR nuclear shielding for the reference has been computed for an optimized geometry of TMS at the spin-orbit relativistic (ZORA) level employing the TZ2P basis set for Si and the same basis set as the central carbon atom for C. The basis set used for H is either the same as the hydrogen atoms of the ligands or TZP in the case of complex **I**.

Structures

In order to assess the influence of computational aspects on the most important structural parameters of the $[Au_6C]^{2+}$ core, results from different density functional calculations have been compared with those from MP2 structure optimizations. In all cases, we have employed basis sets of triple-ζ

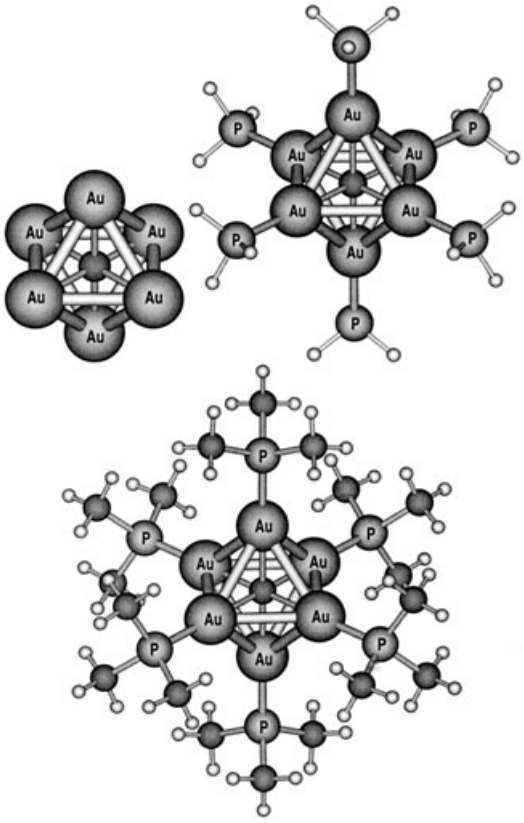

Figure 2. Optimized structures of complexes **I**, $[Au_6C]^{2+}$, **II**, $[(H_3PAu)_6C]^{2+}$, and **III**, $[(Me_3PAu)_6C]^{2+}$. The structures shown here were optimized by using MP2/TZVPP(2f) (**I**), and BP86/TZVPP(2f) (**II**, **III**).

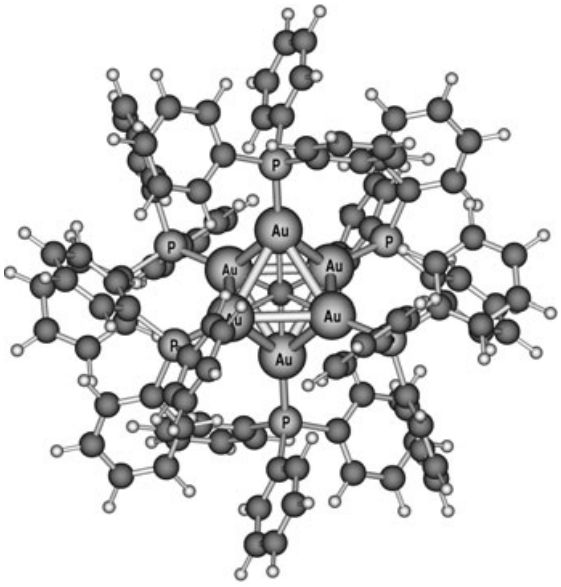

Figure 3. Optimized structure of complex **1**, $[(Ph_3PAu)_6C]^{2+}$. The structure was optimized using BP86/TZVPP(2f)/SVP, that is, we used large TZVPP(2f) basis sets for the $[Au_6C]$ core and the P atoms, and a SVP basis set for the phenyl groups.

valence quality with at least one set of polarization functions.

As already mentioned, calculations have been carried out for three different model complexes of type $[(LAu)_6C]^{2+}$ with ligand L = no ligand (**I**), PH_3 (**II**), and PMe_3 (Me = methyl; **III**), as well as for the experimentally known complex with L = PPh_3 (**1**). The structures of complexes **I** to **III** are displayed in Figure 2, whereas the structure of complex **1** is depicted in Figure 3.

For the bare $[Au_6C]^{2+}$ core (cluster **I**), we have performed MP2 and DFT calculations with the large TZVPP(2f) basis set. Due to the lack of electron-donating ligands, the structure of this model is very compact, with Au–C and Au–Au bond lengths of only 203.5 and 287.8 pm in case of MP2, respectively, showing that this is a poor model for the experimentally known complex with bond lengths of 212.2 to 212.9 pm (Au–C) or 296.0 to 309.0 pm (Au–Au). However, it can serve as a simple model for a comparison of MP2 and DFT methods. While the bond lengths calculated with the VWN functional are in fair agreement with the MP2 results, BP86 overestimates the Au–C distance by 6.7 pm and the Au–Au distance by 9.4 pm compared with MP2.

For the $[(H_3PAu)_6C]^{2+}$ complex, calculations by using BP86/TZVP and MP2/TZVP have been carried out assuming D_{3d} symmetry. As can be seen from the data in Table 1, the MP2 results for the Au–C and Au–Au distances are about 3 and 4.5 pm, respectively, shorter than the bond lengths calculated by using BP86. The Au−P bond lengths are only slightly longer for BP86. It can furthermore be recognized that all Au–C and Au–Au distances within a particular structure are almost equal, the largest variations being 1.3 pm between the longest and the shortest individual Au–Au contact for the BP86/TZVP structure. Variations larger than 0.2 pm for the Au−P bond lengths within a particular complex are not found for any of the structures investigated here. We have also checked the influence of the basis set on the BP86 results in this molecule by performing a BP86/TZVPP(2f) structure optimization. The larger basis set indeed decreases the equilibrium bond lengths for all types of bond lengths investigated here by 1 to 2 pm, bringing the results in better agreement with the MP2/TZVP calculation and with the experimental values.

Another important test on the reliability of structures concerns the point group symmetry of the molecules. Be-

Table 1. Selected calculated bond lengths in pm for complexes $[(LAu)_6C]^{2+}$ with L = no ligand (**I**), PH_3 (**II**), PMe_3 (**III**), PPh_3 (**1**), $PPh_2(p\text{-}C_6H_4NMe_2)$ (**2**), and $[(iPr_3PAu)_6C]^{2+}$ (**4**). Calculations were performed by using the BP86 and VWN density functionals as well as the MP2 method, and TZVP or TZVPP(2f) basis sets. For the complexes **1**, **2**, and **4**, we used SVP basis sets for the phenyl groups.

No.	Model	Ligand L	Method/ basis	Sym.	Au–C	Au–Au	Au–P
1	**I**	(none)	MP2/TZVPP(2f)	O_h	203.5	287.8	–
2	**I**	(none)	BP86/TZVPP(2f)	O_h	210.2	297.2	–
3	**I**	(none)	VWN/TZVPP(2f)	O_h	204.4	289.0	–
4	**II**	PH_3	MP2/TZVP	C_s	214.5	303.3	232.2
5	**II**	PH_3	BP86/TZVP	C_s	to 214.6	to 303.9	to 232.3
5	**II**	PH_3	BP86/TZVP	C_s	217.4	307.2	233.6
					to 217.7	to 308.3	to 233.8
6	**II**	PH_3	VWN/TZVP	C_s	212.1	299.7	228.9
					to 212.4	to 300.8	to 229.0
7	**II**	PH_3	MP2/TZVP	D_{3d}	214.5	303.2	232.2
					to 214.7	to 303.7	to 232.3
8	**II**	PH_3	BP86/TZVP	D_{3d}	217.5	307.2	233.6
					to 217.7	to 308.5	to 233.7
9	**II**	PH_3	BP86/TZVPP(2f)	D_{3d}	216.3	305.5	231.5
					to 216.4	to 306.7	
10	**III**	PMe_3	BP86/TZVPP(2f)	D_{3d}	217.3	306.8	232.5
					to 217.5	to 308.1	
11	**III**	PMe_3	VWN/TZVPP(2f)	D_{3d}	211.5	298.4	227.5
					to 211.6	to 299.9	to 227.6
12	**1**	PPh_3	BP86/TZVPP(2f) /SVP	C_i	217.4	303.2	233.6
					to 217.8	to 312.1	to 233.8
13	**1**	PPh_3	exptl[1]		212.2	296.0	226.9
					to 212.9	to 309.0	to 227.4
14	**2**	$PPh_2(p\text{-}C_6H_4NMe_2)$	BP86/TZVPP(2f) /SVP	–	217.3	301.6	233.6
					to 218.0	to 315.6	to 233.9
15	**4**	$PiPr_3$	BP86/TZVPP(2f) /SVP	–	218.0	300.9	235.1
					to 218.7	to 312.9	to 235.4

sides the D_{3d} symmetric structure described above for cluster **II**, we have also optimized the structure of the $[(H_3PAu)_6C]^{2+}$ complex using MP2/TZVP and assuming C_s symmetry. The energy difference between these two structures is almost negligible, and the structural parameters of the $[Au_6C]^{2+}$ core do not change by more than 0.2 pm compared with the D_{3d} structure. This suggests a small influence of the orientation of the ligands on the core structure, at least for the small PH_3 phosphine ligands. To validate density functional methods for this example: a BP86/TZVP structure optimization yields Au–C and Au–Au bond lengths which are about 3 to 4 pm longer than in the MP2 calculation, and Au–P distances which are about 1.5 pm longer. VWN, on the other hand, leads to bond lengths which are *shorter* than the corresponding MP2 values (about 2 to 3.5 pm for Au–C and Au–Au distances, about 3 to 3.5 pm for Au–P bond lengths). This demonstrates that the systematically shorter VWN bond lengths are not to be preferred over the BP86 data because the decrease in bond length can be too large in our gold cluster structure optimizations.

Since we set out to study the effect of the ligand chosen as a model for the PPh_3 group, we consequently replaced the PH_3 groups with the larger PMe_3. The role of the phosphine ligand in *mononuclear* gold compounds has already been investigated by Häberlen and Rösch[61] with VWN calculations. They have found that in order to obtain structural properties PH_3 is a suitable model for PPh_3, but for energy properties and for the dipole moment the larger PMe_3 ligand should be used instead. The general role of phosphine ligands in gold cluster chemistry (as opposed to the bare Au_x systems) has been studied by Schwerdtfeger and Boyd[62] who have used relativistic SCF and MP2 calculations to trace the electronic effects of the PH_3 phosphine on the gold dimer. In the following, we report results for different phosphine ligands which we have obtained for the *hexanuclear* gold clusters under consideration in this work.

For cluster **III**, reliable calculations with large basis sets were only feasible using density functional methods; the results obtained with the BP86 exchange-correlation functional are given in Table 1. We note that the Au–C and Au–Au bond lengths are increased by about 1.0 or 1.4 pm, respectively, for the BP86 calculation compared with the PH_3 model, which may be attributed to the steric repulsion due to the larger substituents. Also, the Au–P bond lengths are about 1.0 pm longer in the $[(Me_3PAu)_6C]^{2+}$ complex for BP86. Again, the variations in the individual bond lengths of the same type are modest, 1.3 pm between the shortest and the longest Au–Au contact at most. By using the VWN functional instead of BP86 for this compound has a pronounced effect on the bond lengths: the VWN Au–C contacts are between 211.5 and 211.6 pm, while the corresponding BP86 values are between 217.3 and 217.5 pm. Additionally the Au–Au and Au–P distances are about 8 or 5 pm shorter for VWN when compared with the BP86 results. Again, VWN yields considerably shorter bonds for the central $[Au_6C]^{2+}$ core than BP86 and even MP2.

Since the use of GGA functionals such as BP86 is state-of-the-art in DFT calculations of large molecules, and since we do not want to rely on a possible error cancellation within the local density approximation (which does not work well in all cases, see examples above), we used the BP86 exchange-correlation functional for the structure optimization of the large $[(Ph_3PAu)_6C]^{2+}$ complex. This functional yields consistent structural parameters for the different complexes investigated here. The Au–C bond lengths do not change significantly compared to the PMe_3-ligand calculation, and the Au–P distances increase only by about 1.2 pm on average. Also, the average Au–Au distance of about 307 pm is comparable to the model complex with trimethylphosphine ligands, but the variation in the individual bond length ranges from 303.2 pm, which is 3.6 pm shorter than the shortest Au–Au contact in that complex, to 312.1 pm, which is 4.0 pm longer than the longest Au–Au bond length. This agrees with the experimental Au–Au bond length's variation of up to 13 pm.[1] However, even for this model the calculated bond lengths are slightly too long compared to the experimental values (about 5 pm for the Au–C and Au–P distances; the assessment of the Au–Au distances is difficult due to the large variations). We note that these results are in good agreement with previously published calculations.[25]

Additionally, we optimized the structures of the experimentally studied complexes **2** and **4** using the same exchange-correlation functional and basis set as employed for complex **1**. For compound **2**, the Au–C and Au–P bond lengths are very similar to cluster **1**, while the variations in the Au–Au distances are even larger (between 301.6 and 315.6 pm). The P*i*Pr$_3$ ligands in complex **4** lead to Au–C bond lengths which are slightly longer, but still comparable to those of clusters **1** and **2**. Also the Au–P distances are increased by about 1.5 pm compared with these compounds. The Au–Au bond lengths show similar variations as in the cluster with PPh_3 ligands, although the shortest Au–Au contacts are even 2.3 pm shorter than in complex **1**.

NMR Properties

Besides the main goal of this work, namely the investigation of the unexpected range of the ^{13}C NMR chemical shift of the central carbon atom in **1**, it is also important to study the various methodological influences as well as the role played by the ligands in the evaluation of this chemical shift. The issues are as follows: i) the influence of the approximate functionals which have been used, ii) the size of the basis sets, iii) the geometries of the optimized clusters, and iv) the nature of the ligands. The computed NMR results are collected in Tables 2 and 3.

As mentioned in the Section on Computational Details, the VWN functional has been used for most of the NMR calculations because of the generally reasonable accuracy that has been obtained with this functional in previous studies of NMR properties of heavy metal complexes.[23,46,52–59]

Table 2. Calculated NMR shieldings (σ) and chemical shifts (δ)[a] of ^{13}C in the complexes **I**–**III**, **1**, **2**, and **4** (in ppm).

optimized geometry[b]	NMR computational settings: method	basis[c]: C	Au	P	C (lig.)	H	NMR: $\sigma(^{13}C)$	$\delta(^{13}C)$[d]
			complex **I**					
1	VWN	TZ2P	TZ2P	–	–	–	486.8	−302.9
1	VWN	TZ2P	TZ2P (4f)	–	–	–	471.8	−287.9
			complex **II**					
9	VWN	TZ2P	TZ2P (4f)	TZP (2p)	–	DZ	81.4	99.4
9	VWN	TZ2P	TZ2P (4f)	TZP (2p)	–	DZP	79.2	104.0
9	VWN	TZ2P	TZ2P (4f)	TZP (2p)	–	TZP	75.8	108.1
9	VWN	TZ2P	TZ2P	TZP (2p)	–	TZP	74.1	109.8
9	BP[e]	TZ2P	TZ2P	TZP (2p)	–	TZP	83.8	101.1
9	PW[f]	TZ2P	TZ2P	TZP (2p)	–	TZP	85.0	99.6
4	VWN	TZ2P	TZ2P	TZP (2p)	–	TZP	74.4	109.5
7	VWN	TZ2P	TZ2P	TZP (2p)	–	TZP	74.3	109.6
1[g]	VWN	TZ2P	TZ2P	TZP (2p)	–	TZP	41.8	142.1
9	VWN	DZ	TZ2P (4f)	TZP (2p)	–	TZP	100.8	88.3
9	VWN	DZ(1s)	TZ2P (4f)	TZP (2p)	–	TZP	96.0	92.9
9	PW	DZ(1s)	TZ2P (4f)	TZP (2p)	–	TZP	104.7	82.7
			complex **III**					
10	VWN	TZ2P	TZ2P	TZP (2p)	TZP (1s)	TZP	64.6	119.3
10	VWN	TZ2P	TZ2P (4f)	TZP (2p)	DZ (1s)	DZ	66.5	114.3
			complex **1**					
12	VWN	TZ2P	TZ2P (4f)	TZP (2p)	DZ (1s)	DZ	68.2	112.6
12	PW	TZ2P	TZ2P (4f)	TZP (2p)	DZ (1s)	DZ	81.3	99.6
12	VWN	aug-TZ2P	TZ2P (4f)	TZP (2p)	DZ (1s)	DZ	49.9	128.7
			complex **2**					
14	VWN	TZ2P	TZ2P (4f)	TZP (2p)	DZ (1s)	DZ	66.8	114.0
14	VWN	aug-TZ2P	TZ2P (4f)	TZP (2p)	DZ (1s)	DZ	48.5	130.1
			complex **4**					
15	VWN	aug-TZ2P	TZ2P (4f)	TZP (2p)	DZ (1s)	DZ	39.6	139.0

[a] Chemical shifts with respect to TMS. Relativistic (ZORA) computations including spin-orbit coupling. [b] See column 1 of Table 1. [c] Frozen core in parentheses. [d] Basis set for TMS: Si, TZ2P; C, the same as the central carbon atom; H, the same as the hydrogen atoms of the ligands (if not present, TZP). [e] Becke–Perdew functional. [f] Perdew–Wang (PW91) functional. [g] PH_3 ligands added to the optimized geometry of $[Au_6C]^{2+}$. No further geometry relaxation.

In addition, we have applied in some calculations two common GGA density functionals, PW91 and BP86, in order to analyze the dependence of the ^{13}C shielding constant and chemical shift on the approximations in the density functional. For both GGA functionals (BP86 or PW91), a sizable increase of the order of 10 ppm is obtained compared to the ^{13}C shielding constant computed with the VWN functional. This increase is seen to result from changes in the paramagnetic σ^P, the diamagnetic σ^D, and the spin-orbit σ^{SO} contributions. A decrease by approximately the same amount is found for the chemical shift. This is due to the fact that the ^{13}C shielding constant for the reference (TMS) is very similar when computed with the VWN or one of the GGA functionals.

The second issue is the influence of the quality of the basis set on the ^{13}C NMR properties. Several basis sets, in some cases limited by the size of the model clusters, have been applied. In most computations, the same triple-ζ Slater-type basis set augmented with two polarization functions has been employed for the central carbon atom. For the bare $[Au_6C]^{2+}$ core (**I**), freezing the Au core shells up to 4f results in a decrease of 15 ppm of the ^{13}C shielding, due to sizable changes in all terms that contribute to the shielding tensor. For the other complexes, the presence of coordinated ligands around the $[Au_6C]^{2+}$ core is seen to diminish the influence of the frozen core approximation. For instance, without a frozen core for the Au atoms, the ^{13}C chemical shift of the central carbon atom in **II** was computed to be 109.8 ppm whereas with a 4f frozen core, it was computed to be 108.1 ppm. From Table 3, it can be seen that the large ^{13}C shielding in the $[Au_6C]^{2+}$ moiety (**I**) is mainly caused by the σ^{SO} spin-orbit contribution. It results mainly from the spin-orbit coupling in the Au 5d shell. Taking the rather extraordinary magnitude of σ^{SO} in **I** into consideration, a 15 ppm, or less than 10%, contribution from the Au 4f shells seems reasonable. For the complexes **II**, **III**, and **1**, the σ^{SO} contributions are almost completely quenched, mostly due to the electronic effects by the phosphine ligands. We have shown previously that a strongly σ-binding ligand *trans* to a metal–metal bond drastically reduces the (Fermi-contact contribution to the) metal–metal spin–spin coupling constant.[56,57,63] It is therefore not unlikely that a similar effect is in place here that almost completely eliminates the σ^{SO} Fermi contact shielding term when the phosphine ligands are added to the CAu_6^{2+} moiety. The *relative* Au 4f spin-orbit contributions now exceed 10% but are still of the same order of magnitude as in **I** and partially counterbalanced by changes in σ^P (Table 3, rows 5, 6).

A rather spectacular effect on the central carbon's nuclear magnetic shielding is obtained when adding high exponent 1s functions to its basis set (aug-TZ2P). For instance, in complex **1** this increases the chemical shift by 16 ppm (128.7 vs 112.6 ppm). Our motivation of supplying these basis functions originates in the large spin-orbit contributions to the chemical shift in complex **I**. From the computational results it is obvious that for the phosphine complexes these spin-orbit effects are delicately balanced and suppressed mainly by the electronic effects from the ligands. This effect is discussed in more detail below. The balancing must therefore be expected to be sensitive to approximations in the computational model. Because the mechanism for σ^{SO} is—on the side of the light nucleus—essentially the same as for the

Table 3. Individual contributions to the ^{13}C shielding constants in the complexes **I**–**III**, **1**, **2**, and **4**.[a]

No.[b]	σ^P	σ^D	σ^{SO}	Total σ
		complex **I**		
1	−24.5	271.1	240.2	486.8
1	−3.9	264.3	211.5	471.8
		complex **II**		
9	−193.4	281.8	−7.0	81.4
9	−194.7	282.6	−8.7	79.2
9	−196.1	283.1	−11.1	75.8
9	−202.0	284.8	−8.6	74.1
9	−199.7	291.3	−7.7	83.8
9	−197.6	290.0	−7.4	85.0
4	−205.3	287.8	−8.1	74.4
7	−205.4	287.8	−8.1	74.3
1[c]	−244.5	308.2	−21.9	41.8
9	−121.5	228.1	−5.7	100.8
9	−122.1	229.3	−11.2	96.0
9	−119.2	234.3	−10.4	104.7
		complex **III**		
10	−205.5	284.2	−14.2	64.6
10	−197.9	278.6	−14.2	66.5
		complex **1**		
12	−196.9	278.6	−13.6	68.2
12	−189.7	283.3	−12.3	81.3
12	−178.9	252.8	−24.0	49.9
		complex **2**		
14	−198.2	278.5	−13.5	66.8
14	−180.4	252.9	−23.9	48.5
		complex **4**		
15	−195.6	263.4	−28.2	39.6

[a] Small σ^{GC} contributions are included in the individual σ^P and σ^{SO} terms. Computational details are given in Table 2 (same ordering of rows). [b] See column 1 of Table 1. [c] PH_3 ligands added to the optimized geometry of $[Au_6C]^{2+}$. No further geometry relaxation.

Fermi-contact term of nuclear spin–spin coupling[17,23,64,65] it requires steep (high-exponent) s functions for its proper description, in particular in relativistic calculations.[52,53] That there is indeed a sensitive balancing between various competing effects present is also indicated by the data of Table 3. The addition of steep functions does not just cause an increase of the magnitude of σ^{SO} but concomitant changes in σ^D and σ^P of the same order of magnitude. An accurate description of the influence of the Fermi-contact term at the central carbon nucleus also turned out to be essential in order to obtain reasonable agreement with experiment for the central carbon's chemical shift in complex **2** (see end of this Section).

In order to be able to compute ^{13}C NMR properties for the largest complexes, that is, the model cluster **III** and the experimental complexes **1**, **2**, and **4**, we were interested first in the study of the efficiency of the calculations with the smallest basis sets for the C and H ligand atoms. For cluster **II** for instance, changing the basis set of the H atoms of the PH_3 ligands from TZP to DZ produces a decrease of about 9 ppm in the chemical shift (108.1 vs 99.4 ppm). However, for the cluster **III** for which $L=PMe_3$, it seems that using the smallest basis sets for the ligand and Au atoms does not affect as much (around 5 ppm) the chemical shift of the central carbon atom.

The influence of some geometrical parameters (geometry optimizations, and the nature of the ligands) shall also be discussed. For instance, the cluster **II** for which $L=PH_3$, has been optimized by using different methods and basis sets under different symmetries (see the previous Section). Whatever the optimized geometries are, which differ only by small modifications of the bond lengths (see Table 1), the ^{13}C chemical shift is not strongly affected with 109.8, 109.5 and 109.6 ppm for the geometries 9, 4 and 7, respectively.

By using the same basis sets for the NMR computations (TZ2P, TZ2P(4f), TZP(2p), DZ(1s) and DZ for the central carbon atom, the gold and phosphorus atoms, and the carbon and hydrogen atoms of the ligands, respectively), it appears that the presence of the ligands has, as expected, the strongest influence on the chemical shift of the central carbon atom. Without any ligand around the $[Au_6C]^{2+}$ cage (**I**), a large negative chemical shift of −287.9 ppm is computed. As already mentioned, it stems from large shielding spin-orbit (and diamagnetic) contributions to the ^{13}C shielding constant. The addition of a PH_3 ligand on each Au atom (**II**) positively shifts $\delta(^{13}C)$ of the interstitial carbon nucleus (99.4 vs −287.9 ppm). This strong deshielding is caused by a sizable negative σ^P and by a cancellation of σ^{SO}. Replacing the PH_3 ligands (**II**) by PMe_3 (**III**) still quite noticeably affects the chemical shift (114.4 vs 99.4 ppm), whereas a change of less than 2 ppm is observed when the PMe_3 ligands (**III**) are replaced with PPh_3 (**1**). The addition of PH_3 ligands to the $[Au_6C]^{2+}$ core without re-optimization strongly alters the chemical shift from −302.9 to 142.1 ppm. This result shows that the chemical shift of the central carbon atom depends, of course, on the geometrical arrangement of the cluster, but much more strongly on the electronic effect of the ligands on the CAu_6 core. The nearly vanishing paramagnetic shielding and the large σ^{SO} contributions suggest that inside the bare Au_6 cage the central carbon atom mainly sees a nearly spherical strongly shielding environment. The situation is very different when the phosphine ligands are added.

For complex **1**, the chemical shift of the central carbon atom is then computed to be 112.6 ppm with VWN/TZ2P, 99.6 ppm with PW91/TZ2P, and 128.7 ppm with VWN/aug-TZ2P (see Table 2). But, how accurate are these values? From the strong influence of spin-orbit coupling on the central carbon shift it is clear that the aug-TZ2P results are more reliable. As seen before, improving the density functional (GGA vs LDA) reduces the chemical shift, whereas adding polarization functions in the ligand's basis has the opposite effect. Because of the computational costs, complexes **1**, **2**, and **4** could not be studied with a polarized basis on the ligands. From the preceding discussion it is clear that the use of the VWN functional and an unpolarized basis on the ligands provides some significant error cancellation. We therefore suggest that the VWN/aug-TZ2P results for **1** are the ones that should be closest to the experimental data. This is supported by the rather good agreement between calculated and experimental results for complex **2** (see

below), in particular when taking the sensitive balancing of spin-orbit effects in these complexes into consideration.

In order to further investigate the computational errors, we have computed the ^{13}C chemical shift of the carbon atoms of the phenyl groups of the experimental complex **1** and for benzene, by using the same basis sets. Experimentally, the ^{13}C chemical shift of 128.5 ppm for the carbon atoms in benzene is close to the reported shifts of the phenyl ligands in complex **1**. We have computed $\delta(^{13}C)$ for benzene for two geometries, the experimental one ($d_{C-C}=139.9$ pm, $d_{C-H}=110.1$ pm)[66] and an optimized one (BP86/SVP, $d_{C-C}=140.7$ pm, $d_{C-H}=110.2$ pm). The results are collected in Table 4.

Table 4. Calculated NMR shieldings (σ) and chemical shifts (δ)[a] of ^{13}C for the phenyl ligands of the complex **1** and for benzene (in ppm).

	Computational settings			^{13}C NMR		
	method	basis[b]		σ_{calcd}	δ_{calcd}	δ_{exptl}[c]
		C	H			
		phenyl ligand of **1**[d]				
C_{ipso}	VWN	DZ(1s)	DZ	60.8	138.8	129.71
C_{ortho}	VWN	DZ(1s)	DZ	65.0	134.6	133.91
C_{meta}	VWN	DZ(1s)	DZ	68.2	131.4	129.50
C_{para}	VWN	DZ(1s)	DZ	67.1	132.5	132.06
$C_{av.}$[e]	VWN	DZ(1s)	DZ	65.7	133.9	131.43
		benzene (exp. geometry)[f]				
	VWN	DZ(1s)	DZ	71.2	128.4	128.5
	PW	DZ(1s)	DZ	73.0	125.7	128.5
	VWN	DZ	DZ	72.5	127.1	128.5
	VWN	TZP(1s)	DZ	46.0	134.9	128.5
	VWN	TZP	DZ	45.6	135.3	128.5
	VWN	TZ2P	DZ	45.0	135.8	128.5
	VWN	TZ2P	TZP	44.2	139.7	128.5
	PW	TZ2P	TZP	50.5	134.1	128.5
		benzene (opt. geometry)[g]				
	VWN	DZ(1s)	DZ	69.6	130.0	128.5
	PW	DZ(1s)	DZ	71.4	127.3	128.5
	VWN	DZ	DZ	71.0	128.6	128.5
	VWN	TZP(1s)	DZ	44.4	136.5	128.5
	VWN	TZP	DZ	44.1	136.8	128.5
	VWN	TZ2P	DZ	43.4	137.4	128.5
	VWN	TZ2P	TZP	42.7	141.2	128.5
	PW	TZ2P	TZP	48.9	135.7	128.5

[a] Chemical shifts with respect to TMS. Relativistic (ZORA) computations including spin-orbit coupling. [b] Frozen core in parentheses. [c] See refs. [1] (**1**) and [66] (benzene). [d] Averaged results obtained from five phenyl groups. [e] Results averaged on all the carbon atoms of the phenyl ligands. [f] See ref. [66]. [g] Optimized with BP86/SVP. $d_{C-C}=140.7$ pm, $d_{C-H}=110.2$ pm.

The average ^{13}C chemical shift of the carbon atoms of the phenyl ligands in **1** is computed only 2.5 ppm larger than the experimental one with the DZ(1s) basis and the VWN functional (133.9 vs 131.4 ppm). With the same basis and functional, the calculated $\delta(^{13}C)$ in the optimized benzene structure (130.0 ppm) also overestimates the experimental value by only 1.5 ppm. For benzene, an increase of the flexibility of the basis set increases the chemical shift. For instance, with TZ2P and TZP as basis sets for C and H, respectively, the $\delta(^{13}C)$ is more than 10 ppm larger than the experimental one (141.2 vs 128.5 ppm). For all the basis sets, the use of the PW91 functional diminishes the difference between computed and experimental values. With the smallest basis sets, for example, the $\delta(^{13}C)$ decreases from 130.0 to 127.3 ppm. The same trend is observed for the central carbon shift in complex **II** (see Table 2), for which the use of the PW91 functional causes a decrease of 10 ppm of the chemical shift (82.7 vs 92.9 ppm). Thus, the effects on the ^{13}C chemical shift of the use of both the small basis sets and the PW91 functional are of the same order of magnitude in opposite directions. For benzene as well as for the phenyl carbon atoms in **1**, very good agreement with experiment is obtained with the VWN functional and the unpolarized DZ(1s) frozen core basis, which is obviously due to a fortuitous error cancellation. The largest errors are seen to occur for C_{ipso} which indicates the necessity for a higher-quality polarized basis in particular at this position in the ligands of **1**. Very good agreement with experiment is further obtained for benzene with a good quality basis set and a GGA functional. As already mentioned, for the chemical shift of the central carbon atom in **II** and **1** we find effects of similar magnitude and the same sign regarding different basis sets and density functionals.

The presence of steep functions in the basis set of the central carbon atom turned out to be essential. This is further confirmed by the calculation of the chemical shift of the central carbon atom in **2** for which the experimental value is 137.27 ppm. δ_C is computed at 130.1 ppm with the aug-TZ2P basis for the central carbon atom, whereas it is computed at only 114.0 ppm without the additional steep functions. This result indicates that for this particular type of complex, because of the aforementioned cancellation of errors (ligand basis set vs density functional), the calculation with the VWN functional and the steep functions for the central carbon atom offers the best compromise for a good investigation of the experimental ^{13}C NMR chemical shift of the central carbon atom in **1**. As a supplementary test, $\delta(^{13}C)$ of the interstitial carbon atom in **4** has been computed. Owing to the absence of phenyl substituent, the signal is easily detected experimentally at $\delta=154.6$ ppm. The difference between the computed value ($\delta=139.0$ ppm) and the experimental one is larger than for complex **2** for instance. This

deviation can be explained partially by difficulties encountered in obtaining an optimized structure for this complex. However, the ordering of the computed $\delta(^{13}C)$ for the complexes **1**, **2**, and **4**, that is, 128.7 (**1**), 130.1 (**2**), and 139.0 ppm (**4**), respectively, follows the ordering of the experimental data for **2** (137.3 ppm)[14] and **4** (154.6 ppm)[16] and the expected chemical shift for **1** (135.3 ppm).[14]

Besides the sources of errors which were already discussed, remaining errors in the computation can be attributed to yet neglected effects, for instance from vibrations of the central carbon in the Au cage, or surrounding solvent molecules. Because of the sensitive balance between competing effects, it is not easy to point out a clearly dominant source of errors.

Summary and Conclusions

More than ten years ago,[14] experimentalists were expecting that a quantum chemical calculation could give an explanation for the unexpected chemical shift at 137.27 ppm (in the arene region) of the interstitial carbon atom in $[C\{Au[P(C_6H_5)_2(p\text{-}C_6H_4NMe_2)]\}_6]^{2+}$. For instance, the chemical shifts of interstitial carbon atoms in typical carbonyl transition metal carbides appear at about 450 ppm instead.[15] Because of the cage-like environment, a strong magnetic shielding of the central carbon would also not have been very surprising. We find that the suppression of strongly shielding spin-orbit contributions from the Au cage due to electronic effects from the phosphine ligands is responsible here for the unexpected chemical shift. The same is true for complex **1** for which the central carbon's chemical shift could originally not be detected experimentally but has later been assigned to a signal at 135.2 ppm by comparison with data obtained for the related complex **2**.[14] From our computations we confirm that it is in the same range as the one for complex **2**, but slightly smaller by about 1–2 ppm. This in agreement with the experimental values. The best computed chemical shift for **1** at 128.7 ppm underestimates the experimental value ($\delta = 135.2$ ppm) proposed by Schmidbaur et al.[14] by less than 10 ppm.

All the parameters we have studied (functionals, basis sets, ligand effects) influence significantly the chemical shift of the central carbon atom. We have already mentioned that the influence of polarization functions on the ligand atoms can be of the order of 10 ppm. This value is also the difference which can be attributed to the use of a GGA instead of a LDA functional in the calculations. However, it turns out that these effects are to a large extent cancelled out. The total ligand influence is much more significant than these two effects, resulting in a difference of about 400 ppm between the carbon chemical shifts computed for the clusters **I** and **1**, for instance. By considering an error of just 5% in this ligand contribution, the calculations would already be off by about 20 ppm. Therefore, we regard the agreement between calculated and experimental value for complex **2**, and to a lesser extent for complex **4**, as quite satisfactory. Apart from approximations in the functional, the closer to the experimental structure the computational model is, the larger is the calculated chemical shift of the interstitial carbon atom. Therefore, our "best" results underestimate, rather than overestimate, the true experimental value.

A detailed orbital-based analysis of the calculated results would be able to provide further insight into the mechanisms that cause the unexpected chemical shift for the central carbon in **1**, **2**, and **4**. Such analysis functionality is under development in our group. Presently, nuclear shielding from spin-orbit ZORA calculation can unfortunately not be analyzed in the same way as, for example, in the scalar (Pauli) relativistic method developed by Schreckenbach and Ziegler.[50]

Further theoretical investigations on the ^{13}C NMR properties of related gold complexes for which experimental data are missing, in particular $[(Ph_3PAu)_5C]^+$, the pentakis analogue of **1**,[67] are in progress.

Acknowledgement

We are grateful to Professor Pekka Pyykkö for stimulating discussions on relativistic effects in gold clusters. We also greatly appreciate the constructive comments from the anonymous reviewers. J.N. gratefully acknowledges funding by a Kekule-Stipendium of the FCI. J.N. and M.R. acknowledge support from the collaborative research project SFB 583 "Redoxaktive Metallkomplexe". B.L.G. and J.A. acknowledge support from the Center for Computational Research (CCR) at SUNY Buffalo. Further, a subset of the computations were performed as part of the Molecular Sciences Computing Facility (MSCF) Grand Challenge project entitled "Reliable Electronic Structure Calculations for Heavy Element Chemistry: Molecules Containing Actinides, Lanthanides, and Transition Metals" at the Environmental Molecular Sciences Laboratory (a national scientific user facility sponsored by the U.S. DOE Office of Biological and Environmental Research) located at Pacific Northwest National Laboratory.

[1] F. Scherbaum, A. Grohmann, B. Huber, C. Krüger, H. Schmidbaur, *Angew. Chem.* **1988**, *100*, 1602–1604; *Angew. Chem. Int. Ed. Engl.* **1988**, *27*, 1544–1546.
[2] J. Autschbach, B. A. Hess, M. P. Johansson, J. Neugebauer, M. Patzschke, P. Pyykkö, M. Reiher, D. Sundholm, *Phys. Chem. Chem. Phys.* **2004**, *6*, 11–22.
[3] V. G. Albano, D. Braga, S. Martinengo, *J. Chem. Soc. Dalton Trans.* **1981**, 717–720.
[4] V. G. Albano, M. Sanson, P. Chini, S. Martinengo, *J. Chem. Soc. Dalton Trans.* **1973**, 651–655.
[5] M. R. Churchill, J. Wormald, *J. Chem. Soc. Dalton Trans.* **1974**, 2410–2415.
[6] J. S. Bradley, G. B. Ansell, M. E. Leonowicz, E. W. Hill, *J. Am. Chem. Soc.* **1981**, *103*, 4968–4970.
[7] P. F. Jackson, B. F. G. Johnson, J. Lewis, J. N. Nicholls, M. McPartlin, W. J. H. Nelson, *J. Chem. Soc. Chem. Commun.* **1980**, 564–566.
[8] T. P. Fehlner, P. T. Czech, R. F. Fenske, *Inorg. Chem.* **1990**, *29*, 3103–3109.
[9] R. Khattar, T. P. Fehlner, Czech, P. T. *New J. Chem.* **1991**, *15*, 705–711.
[10] M. Kaupp, *Chem. Commun.* **1996**, 1141–1142.
[11] J. D. Harris, T. Hughbanks, *J. Am. Chem. Soc.* **1997**, *119*, 9449–9459.
[12] J. Shen, T. Hughbanks, *J. Phys. Chem. A* **2004**, *108*, 350–357.
[13] A. Görling, N. Rösch, D. E. Ellis, H. Schmidbaur, *Inorg. Chem.* **1991**, *30*, 3986–3994.

[14] H. Schmidbaur, B. Brachthäuser, O. Steigelmann, *Angew. Chem.* **1991**, *103*, 1552–1553; *Angew. Chem. Int. Ed. Engl.* **1991**, *30*, 1488–1490.
[15] B. F. G. Johnson, J. Lewis, W. J. H. Nelson, J. N. Nichols, M. D. Vargas, *J. Organomet. Chem.* **1983**, *249*, 255–272.
[16] H. Schmidbaur, B. Brachthäuser, O. Steigelmann, H. Beruda, *Chem. Ber.* **1992**, *125*, 2705–2710.
[17] M. Kaupp, "Relativistic effects on NMR chemical shifts" in *Relativistic electronic structure theory*, *Vol. 2* (Ed.: P. Schwerdtfeger), Elsevier, Amsterdam, **2004**.
[18] M. Kaupp, V. G. Malkin, O. L. Malkina, "NMR of transition metal compounds" in *Encyclopedia of Computational Chemistry* (Ed.: P. von Rague Schleyer), Wiley, Chichester, **1998**.
[19] G. Schreckenbach, T. Ziegler, *Theor. Chem. Acc.* **1998**, *99*, 71–82.
[20] M. Bühl, M. Kaupp, O. L. Malkina, V. G. Malkin, *J. Comput. Chem.* **1999**, *20*, 91–105.
[21] J. Autschbach, T. Ziegler, *Coord. Chem. Rev.* **2003**, *238*/239, 83–126.
[22] M. Bühl, "NMR of transition metal compounds" in *Calculation of NMR and EPE Parameters* (Eds.: M. Kaupp, M. Bühl, V. G. Malkin), Wiley-VCH, Weinheim, **2004**.
[23] J. Autschbach, T. Ziegler, "Relativistic Computation of NMR Shieldings and Spin–Spin Coupling Constants" in *Encyclopedia of Nuclear Magnetic Resonance*, *Vol. 9* (Eds.: D. M. Grant, R. Harris), Wiley, Chichester, **2002**.
[24] J. Autschbach, "The calculation of NMR parameters in transition metal complexes" in *Principles and Applications of density functional theory in inorganic chemistry I*, *Structure and Bonding Series, Vol. 112* (Eds.: N. Kaltsoyannis, J. E. McGrady), Springer, Heidelberg, p. 1–48, **2004**.
[25] J. Neugebauer, M. Reiher, *J. Comput. Chem.* **2004**, *25*, 587–597.
[26] R. Ahlrichs, M. Bär, M. Häser, H. Horn, C. Kölmel, *Chem. Phys. Lett.* **1989**, *162*, 165–169.
[27] P. Pyykkö, Y. Zhao, *Angew. Chem.* **1991**, *103*, 622–623; *Angew. Chem. Int. Ed. Engl.* **1991**, *30*, 604–60.
[28] P. Pyykkö, N. Runeberg, *J. Chem. Soc. Chem. Commun.* **1993**, 1812–1813.
[29] P. Pyykkö, N. Runeberg, F. Mendizabal, *Chem. Eur. J.* **1997**, *3*, 1451–1457.
[30] P. Pyykkö, F. Mendizabal, *Inorg. Chem.* **1998**, *37*, 3018–3025.
[31] P. Pyykkö, T. Tamm, *Organometallics* **1998**, *17*, 4842–4852.
[32] D. Andrae, U. Häußermann, M. Dolg, H. Stoll, H. Preuß, *Theor. Chim. Acta* **1990**, *77*, 123–141.
[33] A. D. Becke, *Phys. Rev. A* **1988**, *38*, 3098–3100.
[34] J. P. Perdew, *Phys. Rev. B* **1986**, *33*, 8822–8824.
[35] S. H. Vosko, L. Wilk, M. Nusair, *Can. J. Phys.* **1980**, *58*, 1200–1211.
[36] K. Eichkorn, O. Treutler, H. Öhm, M. Häser, R. Ahlrichs, *Chem. Phys. Lett.* **1995**, *240*, 283–290.
[37] K. Eichkorn, F. Weigend, O. Treutler, R. Ahlrichs, *Theor. Chem. Acc.* **1997**, *97*, 119–124.
[38] A. Schäfer, C. Huber, R. Ahlrichs, *J. Chem. Phys.* **1994**, *100*, 5829–5835.
[39] A. Schäfer, H. Horn, R. Ahlrichs, *J. Chem. Phys.* **1992**, *97*, 2571–2577.
[40] E. J. Baerends, et al. "Amsterdam Density Functional, Theoretical Chemistry, Vrije Universiteit, Amsterdam", URL http://www.scm.com.
[41] C. Fonseca Guerra, O. Visser, J. G. Snijders, G. teVelde, E. J. Baerends, "Parallelisation of the Amsterdam Density Functional program Program" in *Methods and Techniques for Computational Chemistry*, STEF, Cagliari, **1995**.
[42] G. teVelde, F. M. Bickelhaupt, E. J. Baerends, S. J. A. van Gisbergen, C. Fonseca Guerra, J. G. Snijders, T. Ziegler, *J. Comput. Chem.* **2001**, *22*, 931–967.
[43] S. K. Wolff, T. Ziegler, E. van Lenthe, E. J. Baerends, *J. Chem. Phys.* **1999**, *110*, 7689–7698.
[44] E. van Lenthe, E. J. Baerends, J. G. Snijders, *J. Chem. Phys.* **1993**, *99*, 4597–4610.
[45] K. Dyall, E. van Lenthe, *J. Chem. Phys.* **1999**, *111*, 1366–1372.
[46] J. Autschbach, E. Zurek, *J. Phys. Chem. A* **2003**, *107*, 4967–4972.
[47] J. Autschbach, *Theor. Chem. Acc.* **2004**, *112*, 52–57.
[48] E. van Lenthe, A. van der Avoird, P. E. S. Wormer, *J. Chem. Phys.* **1998**, *108*, 4783–4796.
[49] R. Ditchfield, *Mol. Phys.* **1974**, *27*, 789–807.
[50] G. Schreckenbach, T. Ziegler, *Int. J. Quantum Chem.* **1997**, *61*, 899–918.
[51] G. Schreckenbach, *Theor. Chem. Acc.* **2002**, *108*, 246–253.
[52] J. Autschbach, T. Ziegler, *J. Chem. Phys.* **2000**, *113*, 936–947.
[53] J. Autschbach, T. Ziegler, *J. Chem. Phys.* **2000**, *113*, 9410–9418.
[54] J. Autschbach, T. Ziegler, *J. Am. Chem. Soc.* **2001**, *123*, 3341–3349.
[55] J. Autschbach, T. Ziegler, *J. Am. Chem. Soc.* **2001**, *123*, 5320–5324.
[56] J. Autschbach, C. D. Igna, T. Ziegler, *J. Am. Chem. Soc.* **2003**, *125*, 1028–1032.
[57] J. Autschbach, C. D. Igna, T. Ziegler, *J. Am. Chem. Soc.* **2003**, *125*, 4937–4942.
[58] J. Autschbach, B. Le Guennic, *J. Am. Chem. Soc.* **2003**, *125*, 13585–13593.
[59] J. Autschbach, B. Le Guennic, *Chem. Eur. J.* **2004**, *10*, 2581–2589.
[60] J. P. Perdew, J. A. Chevary, S. H. Vosko, K. A. Jackson, M. R. Pederson, D. J. Singh, C. Fiolhais, *Phys. Rev. B* **1992**, *46*, 6671–6687.
[61] O. D. Häberelen, N. Rösch, *J. Phys. Chem.* **1993**, *97*, 4970–4973.
[62] P. Schwerdtfeger, P. D. W. Boyd, *Inorg. Chem.* **1992**, *31*, 327–329.
[63] B. Le Guennic, K. Matsumoto, J. Autschbach, *Magn. Res. Chem.* **2004**, *42*, S99–S116.
[64] Y. Nomura, Y. Takeuchi, N. Nakagawa, *Tetrahedron Lett.* **1969**, 639–642.
[65] M. Kaupp, O. L. Malkina, V. G. Malkin, P. Pyykkö, *Chem. Eur. J.* **1998**, *4*, 118–126.
[66] *CRC Handbook of Chemistry and Physics*, CRC Press LCC, Boca Raton, Florida, 83rd ed., **2003**.
[67] F. Scherbaum, A. Grohmann, G. Müller, H. Schmidbaur, Angew. Chem. **1989**, *101*, 464–466; *Angew. Chem. Int. Ed. Engl.* **1989**, *28*, 463–465.

Received: March 31, 2004
Revised: September 2, 2004
Published online: January 24, 2005